PHYSICAL REVIEW E VOLUME 49, NUMBER 1 JANUARY 1994

Adsorption of line segments on a square lattice

B. Bonnier, M. Hontebeyrie, Y. Leroyer,* C. Meyers, and E. Pommiers
Laboratoire de Physique Théorique, Université de Bordeaux I, 19 rue du Solarium, F-33175 Gradignan Cedex, France
(Received 20 July 1993)

We study the deposition of line segments on a two-dimensional square lattice. The estimates for the coverage at jamming obtained by Monte Carlo simulations and by seventh-order time-series expansion are successfully compared. The nontrivial limit of adsorption of infinitely long segments is studied, and the lattice coverage is consistently obtained using these two approaches.

PACS number(s): 05.70.Ln, 68.10.Jy

I. INTRODUCTION

Random sequential adsorption (RSA) has been used for a long time as a model of irreversible deposition processes [1,2]. An object of a given shape is placed randomly on a substrate, subject to the constraint that it does not overlap previously deposited objects. One determines the coverage, defined as the fraction of area covered by the adsorbed objects, as a function of time, and its infinite-time limit, called the jamming limit. These quantities can be determined exactly in one dimension and by approximate methods or numerical simulations in higher dimensions. The RSA models are characterized by two main parameters: the nature of the substrate—discrete or continuous—and the shape of the deposited objects. Although lattice models are less directly connected with experimental situations, they are easily accessible to numerical simulations and accurate results can be obtained from them. Furthermore, in most cases, one can define a *scaling limit* which allows an extrapolation to the continuum. The jamming limit for the deposition of k-mers on a one-dimensional lattice has been known exactly for a long time [3] as well as its continuum limit [4]. In two dimensions, the regular objects that fit a square lattice are rectangles of width w and length ℓ expressed in units of the lattice spacing. When the aspect ratio α, defined as the length-to-width ratio, varies from 1 to ∞ the shape of the objects changes from the square to the line segment. The continuum limit of aligned squares, taken by letting the edge size approach infinity with the aspect ratio fixed to one, has been studied by Privman, Wang, and Nielaba [5] and by Brosilow *et al.* [6] in the framework of an extensive numerical simulation, leading to an accurate determination of the saturation coverage and of the correlation functions. On the other hand, the deposition of randomly oriented rectangles in the continuum has received much attention in order to guess the influence of the aspect ratio on the kinetics of the process and on its jamming limit [7–9]. For instance, it has been shown that in the case of extremely elongated objects, the jamming coverage approaches zero as a power of the inverse of the aspect ratio. In the limit of an infinite aspect ratio which corresponds to the deposition of *randomly oriented* line segments, the time evolution of the density of deposited segments is driven by a power-law behavior [7,10–12].

RSA of dimers or of small k-mers on the lattice, being one of the simplest two-dimensional process, has been widely studied as a testing model for the approximation methods and numerical simulations. In contrast to the continuum case, the RSA of long segments on a bidimensional lattice has not yet been systematically investigated [13] and this is the problem we address in this paper. The study of such systems can give insight into experimental situations involving the deposition of rectanglelike objects with a large aspect ratio. For example, the sticking of rodlike polymers to a surface on which the activated sites form a lattice [14] may be modeled by an RSA process. In addition, in the limit of infinite segment length, this model is equivalent to the continuum deposition of *aligned* unit segments onto the plane, which is to be compared to the case of *randomly oriented* ones.

We first attack the problem by means of an extensive numerical simulation, which is presented in Sec. II of this paper, where we give the technical details and the analysis of finite-size effects and propose an expression for the large-k behavior of the jamming limit. Then, in Sec. III, we derive seventh-order time-series expansion of the coverage analytically in k and compare the result of the extrapolation at jamming with the asymptotic value obtained by the simulation. We comment on our results in Sec. IV.

II. NUMERICAL SIMULATION

A. Method

We consider a periodic square lattice of linear size L, on which we randomly deposit line segments of k sites (k-mers). Since we are interested in the limit of long segments, we need a large-scale simulation. However, the standard method usually implemented in the continuum

*Electronic address: Leroyer @FRCPN11.IN2P3.FR

deposition of oriented squares [6], of dividing the lattice into cells containing at most one object, is not efficient here. Therefore, due to memory storage and computing time limitations, we had to restrict our simulation to segments of length $k \leq 512$ sites on lattices of linear size $L \leq 4096$, preserving in all cases a ratio $L/k \geq 8$. A subsequent study of finite-size effects allows us to make a reliable extrapolation to the $k \to \infty$ limit. This point will be discussed below.

The time evolution to the jamming limit is divided in two regimes [5]: in the initial stage the possible adsorption site is randomly chosen among *all* the sites; in the late stage, it is drawn from the list of vacant positions, which is regularly updated after a fixed number of depositions. The relative duration of both stages is optimized in such a way that the rejection rate in the first stage remains low whereas in the second stage the list of vacant positions is small enough for the updating procedure to be short. Good balance between these constraints is realized for a number of attempts during the first stage of typically four to five times the total number of sites.

For the largest lattice sizes, the memory storage needed is very large. We use multispin coding to store the occupancy state of each site and initialize the list of vacant positions only at the beginning of the second stage when it is reduced to less than 5% of the total number of sites.

Finally, the sample used for averaging and for the error analysis consists of at least 100 independent runs. Although rather small, this sample size leads to results of sufficient accuracy for our purpose.

B. Finite-size effects

Finite-size effects are exactly known in one dimension [15,16]. MacKenzie has shown that, for RSA of k-mers at jamming, the number of vacant sites on a lattice of L sites with open boundary conditions is given by

$$V_L(k) = (k+L)\left[\bar{V}(k) + O\left(\frac{1}{(L/k)!}\right)\right] \quad \text{for } L \to \infty, \quad k/L \to 0$$

where $\bar{V}(k)$ does not depend on L. A *periodic* lattice of L sites, once the first segment is deposited, becomes an open one of $L-k$ sites and the coverages for both systems are related by [where the superscript (O) stands for "open" and (P) for periodic]

$$\Theta_L^{(P)}(k) = 1 - \frac{V_L^{(P)}(k)}{L} = 1 - \frac{V_{L-k}^{(O)}(k)}{L} = \bar{V}(k) + O\left(\frac{1}{(L/k)!}\right).$$

It follows that finite-size corrections are less than exponentially small for a periodic lattice. Although this argument cannot be directly extended to higher dimensions we expect that in two dimensions, the edge effects on the jamming limit on a *periodic* lattice decrease very rapidly when $L \to \infty$ and $k/L \to 0$.

Actually, Privman *et al.* [5] and Brosilow *et al.* [6] have already observed that finite-size effects are negligible for the deposition of oriented squares on periodic lattices of size as small as eight times the square edge. In our case, however, in order to reach the large segment limit at lowest computing cost, we consider systems whose size is not very large compared to the size of the adsorbed segments. For this reason we must handle carefully the finite-size effects. To estimate them, we perform the following analysis. For a given lattice size L, we measure $\Theta_L(k)$ for various values of k up to $k \simeq L/2$ and then repeat this measure for a larger value of L. Figure 1 shows the results for $L = 128$ and $L = 256$. It is apparent that both lattices give the same result for $k \leq 42$. The finite-size effects then start to occur for the $L = 128$ lattice whereas they appear only for $k \geq 90$ for the largest lattice. The continuous line results from the extrapolation discussed in Sec. II C. It thus appears that a lattice of a given size L behaves as if it were infinite as long as the segment size does not exceed at most a quarter of the lattice edge. With this rough analysis as a guide, we have measured $\Theta_L(k)$, using several lattice sizes (typically three to four values) for each k value, up to $L/k = 4$ and check that for the largest sizes, the measured coverages remain consistently within the error bars. We give the results in Table I, which will be used as the basis of our extrapolation of Sec. II C.

Another issue concerning the finiteness of the system is the standard deviation over the sample of the fraction of occupied sites, defined by

$$\sigma_\Theta = \sqrt{\langle \Theta^2 \rangle - \langle \Theta \rangle^2}$$

and connected to the statistical error of the jamming coverage, $\Delta\Theta = \sigma_\Theta / \sqrt{N_s}$, where N_s is the sample size. On the basis of standard statistical arguments, if one assumes that the fluctuations of Θ are driven by the variations of the number of deposited objects, one expects

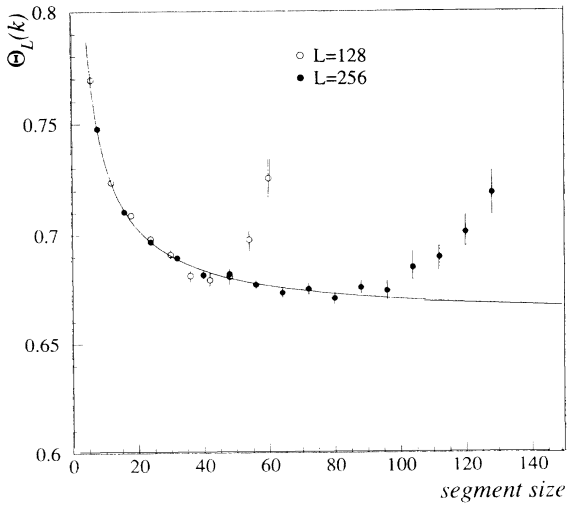

FIG. 1. The jamming limit for the deposition of k-mers on lattice of size $L = 128$ (open circles) and $L = 256$ (filled circles) as a function of k. The solid line corresponds to the best fit of the $L \to \infty$ values.

TABLE I. The jamming limit for the deposition of k-mers on lattice of size L, for various segment lengths k.

k \ L	128	256	512	1024	1536	2048	3072	4096
2	0.9066(2)	0.9068(1)						
4	0.8109(3)	0.8106(2)	0.8106(1)					
8	0.7487(6)	0.7484(3)	0.7477(1)	0.7477(1)				
12	0.7233(8)	0.7239(4)	0.7239(2)					
16	0.7107(13)	0.7111(6)	0.7106(2)	0.7110(1)				
24	0.6956(6)	0.6970(7)	0.6968(4)	0.6967(2)				
32	0.6867(23)	0.6894(13)	0.6890(7)	0.6893(4)				
48		0.6812(20)	0.6814(9)	0.6809(5)				
64		0.6721(25)	0.6769(13)	0.6765(6)				
96	0.6709(38)	0.6734(20)	0.6731(6)	0.6714(5)				
128			0.6697(24)	0.6692(13)		0.6682(6)		
192					0.6656(13)		0.6655(7)	
256				0.6608(27)		0.6641(10)		0.6637(6)
384							0.6632(13)	0.6634(6)
512								0.6628(9)

σ_Θ to decrease as the inverse square root of this number, which would give a behavior in $\sqrt{k}/L$. Instead, for the whole set of data, we observe that

$$\sigma_\Theta(k, L) \simeq 0.1 \, \frac{k}{L} \, .$$

This behavior emerges clearly from Table II, where σ_Θ measured for several fixed k/L is roughly independent of the lattice size L, the constant value obtained for each k/L being proportional to k/L. It is confirmed in Fig. 2 where the k dependence of σ_Θ for $L = 256$ appears to be linear. On the same plot, we have superimposed some data for $L = 512$ and $k = 16, 32, 64, 128$ which coincide within the error bars with the $L = 256$ data for $k = 8, 16, 32, 64$, respectively. The L dependence of σ_Θ is a common feature of all the RSA simulations [1] whereas a linear k dependence is somewhat unexpected. This result can be interpreted as an indication that in the limit of long segments, the system behaves mainly as a one-dimensional one along each direction, the fluctuations being linked to the number of deposited objects *along each line* $(L/k)^2$.

C. The extrapolation

Following the finite-size effect analysis of Sec. II B, we consider that for each segment length k, the value of $\Theta_L(k)$ measured on the largest lattice size L of Table I is a good estimate of $\Theta_\infty(k) = \lim_{L\to\infty} \Theta_L(k)$. These data, plotted as a function of k, are displayed in Fig. 3 for $k \geq 24$. In order to extrapolate to $k \to \infty$, we must guess the large-k behavior. Analogous analyses have been performed previously in one dimension [15] and in two dimensions for the deposition of squares [2,6]. In both cases the large-k limit corresponds to the continuum limit and is approached up to a $1/k$ corrective term.

Although our data exclude a single $1/k$ dependence, they are quite compatible with a superposition of $1/k$ and $1/k^2$ corrective terms. The best fit according to this behavior, realized for $k \geq 48$, is displayed in Fig. 3 and corresponds to the expression

$$\Theta_\infty(k) = 0.660 + 1.071 \, \frac{1}{k} - 3.47 \, \frac{1}{k^2} \qquad (1)$$

from which we conclude that

$$\Theta_\infty(\infty) = 0.660 \pm 0.002, \qquad (2)$$

where the error bar results from a variation of the fitting interval. Accordingly, the coefficents of $1/k$ and $1/k^2$ in Eq. (1) vary in the ranges $[0.85, 1.08]$ and $[-1.0, -3.7]$, respectively.

Let us finally discuss how the jamming coverage varies with the deposition mechanism. Actually, besides the conventional deposition mechanism used here, one can

TABLE II. The standard deviation σ_Θ of the coverage for different fixed values of L/k as a function of the lattice size.

$\frac{L}{k}$ \ L	64	128	256	512	1024
32	0.0038(2)	0.0034(2)	0.0030(2)	0.0024(2)	0.0031(3)
16	0.0070(3)	0.0060(3)	0.0060(3)	0.0059(4)	0.0061(4)
8	0.0125(4)	0.0122(4)	0.0119(7)	0.0117(8)	0.0129(7)
4	0.0247(9)	0.0251(13)	0.0235(9)	0.0265(10)	0.0267(16)

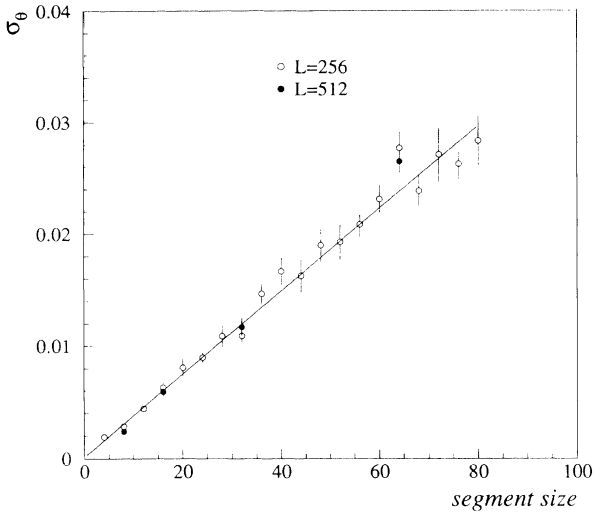

FIG. 2. The standard deviation σ_Θ as a function of the segment size k for the $L = 256$ (open circles) and $L = 512$ (filled circles) lattice sizes. The solid line is the best fit of the $L = 256$ data by a linear function.

choose the so-called "end-on" mechanism in which, once a vacant site has been found, the deposition is (randomly) attempted in *all the directions* until the segment is adsorbed or rejected. This method leads to denser configurations than the conventional one [17] for small k-mers, and for infinitely long k-mers we quote here the coverage from Manna and Švrakić [13]:

$$\Theta_\infty(k) = 0.583(\pm 0.010) + 0.32\,\frac{1}{\ln k} \quad ,$$

clearly smaller than our result, Eq. (2). Comparing both types of data, we observe a crossover for $k \simeq 16$, our saturation coverage becoming larger than the end-on one above this value. Let us point out that the same kind of crossover between conventional and end-on coverages has been observed recently in one dimension [18] at $k = 4$.

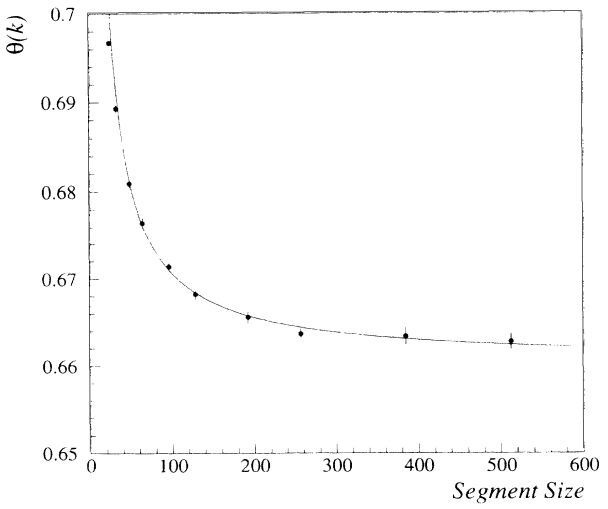

FIG. 3. The estimated $L \to \infty$ jamming coverage as a function of the segment size k and the fit of these data.

III. PERTURBATIVE k-MER FILLING OF THE SQUARE LATTICE

A. The perturbative expansion

We will determine the time-series expansion of the coverage $\Theta(k,t)$ for the RSA of k-mers on a two-dimensional square lattice. The segment orientation is chosen at random with equal probability for horizontal and vertical deposition.

We first construct an operator which realizes the sequential addition process of arbitrary objects on a lattice. This elementary time-evolution operator is obtained by a generalization of the quantum-mechanical methods used by Fan and Percus [19], and by Dickman, Wang, and Jensen [20] to the deposition of arbitrary objects, and cannot be evaluated except in a perturbative way.

The perturbative expansion (PE) of $\Theta(k,t)$ is then

$$\Theta(k,t) = 2k \sum_{n=1} C_n(k)\,\frac{(-1)^{n-1}}{n!}\,t^n, \qquad (3)$$

where the first-order term in time is $2kt$, because the first adsorption attempt on an empty lattice is always accepted and occupies k sites in the two possible orientations, and where the coefficients $C_n(k)$ are given by implicit overlap integrals:

$$C_n(k) = \prod_{i=2}^{n}\left(1 - \prod_{j=1}^{i-1}(1 - K_{ij})\right), \quad n \geq 2 \quad . \qquad (4)$$

The set of integration variables defining a deposition is denoted by i, and $-K_{ij}$ is a hard Mayer function ($K_{ij} = 1$ only if i and j are overlapping objects, 0 otherwise).

The inclusion-exclusion sequence generated by Eqs. (3) and (4) has already been used for square deposition in the continuum [20,21]. Similar techniques appear in hard-sphere modelization of simple liquids at equilibrium [20,22].

Next, one generates the nth-order diagrams by the full expansion of $C_n(k)$. All monomials of this polynomial are connected labeled graphs which are regrouped in classes $\Gamma_{n,i}$ (unlabeled graphs) of the same topology which thus appear with combinatorial weights as can be easily seen in Fig. 4, which shows the first terms of the graphical perturbative expansion.

Let us stress the generality of the above perturbative approach, which is valid for any standard RSA process. The details of the process affect only the graph integrals $I(\Gamma_{n,i})$.

In order to compute $I(\Gamma_{n,i})$, one has to do the summation over $\{x_l\}$, the n vertices of the graph $\Gamma_{n,i}$. Here the vertices $\{x_1, x_2, \ldots, x_n\}$ are to be understood as the position of the starting point and the orientation of each of the n k-mers.

Finally, the graph contribution is

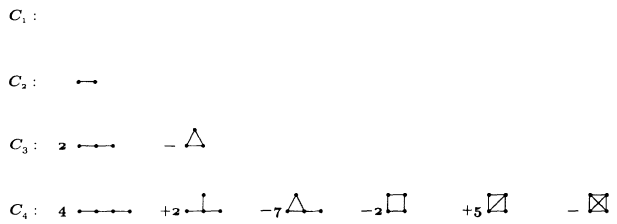

FIG. 4. Graphical expansion of C_n for one, two, three, and four points. The reduction of the number of graphs operated by the topological identification is especially efficient at large orders not depicted on this figure, e.g., at seventh order, $\sim 6 \times 10^5$ labeled graphs are regrouped into $\sim 10^3$ unlabeled ones.

$$I(\Gamma_{n,i}) = \sum_{\{x\}} \prod_{p} K(x_{l_p}, x_{m_p}), \tag{5}$$

where the product $\prod_p$ is done on the links of $\Gamma_{n,i}$ and the sum is over all the degrees of freedom for the k-mer variable x_l, except one which can be frozen at the origin by transational invariance.

Aligned object deposition is of practical interest here because, due to the factorization property of hard Mayer functions [23], it allows us to reduce the problem of two-dimensional integration to a one-dimensional one, once the orientations of the k-mers are fixed. Such a factorization has already been used in the RSA of aligned hypercubes to determine the time series [20,21] and proved to be essential in the study of the Palásti conjecture [21]. In practice, we have analytically calculated all the 2^n projected one-dimensional graph integrals appearing at order n. Sums of products of two one-dimensional integrals are then performed to algebraically obtain the two-dimensional graph integrals for segment deposition.

We have thus stored all the one-dimensional graph integrals $I_{n,i}$ and weights necessary to compute $C_n(k)$ analytically in k, up to the seventh order in t. The analytic expression of graph integrals has no physical interest and we give in Table III the coefficients needed to reconstruct to seventh order the time series expansion of which the first terms are

$$\Theta(k,t) = 2k \left(t - (-1 + 2k + k^2) \frac{t^2}{2} + (1 - 5k + k^2 + 5k^3 + 2k^4) \frac{t^3}{6} + \cdots \right). \tag{6}$$

We give, as a first attempt at resummation, the predictions for the dimer jamming coverage Θ_∞ from one of the more stable methods for computing the infinite time limit of $\Theta(2,t)$, knowing the exponential behavior of the coverage at large times on the lattice.

We first invert the PE, Eq. (3), into a power series of Θ to calculate e^t in terms of Θ. The poles of the Padé approximants formed from this series in Θ give jamming values Θ_∞, which are reached with the expected exponential behavior $\Theta(t) \simeq \Theta_\infty - Ae^{-t}$, the coefficient A being given by the residue. The resulting Padé tables of Θ_∞ of the coefficients A can be found in Table IV, where we notice very good agreement between simulations and time-series estimates of the jamming coverage. In fact, this series for deposition of small size objects can be numerically performed at larger orders than the generic case of k-mer deposition and allows us to observe a wider Padé table.

TABLE III. This table gives the coefficients α_n^p allowing us to reconstruct the seventh-order time-series expansion of $\Theta(k,t)$, the lattice coverage by segments of k sites, by $\Theta(k,t) = 2k \sum_{n=1} \frac{(-1)^{n-1}}{n!} C_n t^n$, in which $C_n = \sum_{p=0}^{2n-2} \alpha_n^p k^p$. For small k-mers, more orders can easily be computed: $k = 2, C_8 = 73\,035\,123, C_9 = 1\,663\,498\,315$, and for $k = 3, C_8 = 20\,554\,179\,608$.

$p \backslash n$	1	2	3	4	5	6	7
k^0	1	-1	1	-9	18	-900	8100
k^1		2	-5	84	-276	20940	-269460
k^2		1	1	-95	645	-79802	1459620
k^3			5	-141	343	46090	-3561354
k^4			2	22	-323	-88615	11703689
k^5				165	-2288	648530	-33506220
k^6				46	529	-365541	16916830
k^7					1357	-745840	59786163
k^8					283	235865	-43362258
k^9						307480	-40950720
k^{10}						50593	16739500
k^{11}							13706391
k^{12}							1848119

The quality of the results, linked to the dispersion of the Padé table, decreases with the length of the k-mer. For example, the same method applied to the eighth-order trimer series is still predictive, giving $\Theta_\infty = 0.842(2)$, and $A = 0.135(5)$ in agreement with both the result of Evans and Nord [24], i.e., 0.8465 obtained by hierarchy truncation which exploits empty site shielding, and the Monte Carlo simulation result of Nord [17], 0.8465(2). For $k \geq 4$, numerous instabilites forbid reliable evaluations.

These instabilities are reminiscent of the problems encountered in summing up the RSA series of $(k \times k)$ squares deposition on a square lattice as k increases: the effective behavior of the truncated power series seems to change, as k increases, from e^{-t} to $\ln t/t$, which prevents the use of a simple and stable extrapolation procedure in the intermediate-k range. The situation is even worse for the deposition of long k-mers because the usual scaling argument does not hold in such a way that the infinite-k limit of the time-series expansion of the coverage cannot be taken order by order. This can then be seen in the behavior of the series for large k,

$$\Theta(k,t) \simeq \frac{1}{k} \sum_{n \geq 1} N_n \quad (k^2 t)^n, \qquad k \gg 1, \tag{7}$$

which implies either $\Theta(k,\infty) = O(1/k)$ or the divergence of the sum.

TABLE IV. Padé table of the dimer jamming coverage obtained through equating $\exp t$ to the Padé approximants $[N(\Theta), D(\Theta)]$ where the denominator D (numerator N) degree varies horizontally (vertically), respectively. For each entry of part (a) the coefficient A of the approach to the jamming limit given by $\Theta \simeq \Theta_\infty - Ae^{-t}$ has been computed through the residue of the corresponding pole and can be found in part (b). For comparison we recall the simulation estimates of 0.9069(2) from Nord [17] and of 0.9068(1) from Table I.

N \ D	1	2	3	4	5	6	7	8
				(a)				
1	1	0.94007	0.92212	0.91478	0.91127	0.90943	0.90841	0.90781
2	0.94117	0.91535	0.91011	0.90826	0.90750	0.90716	0.90699	
3	0.92307	0.91015	0.90781	0.90718	0.90696	0.90688		
4	0.91549	0.90831	0.90718	0.90692	0.90686			
5	0.91179	0.90753	0.90696	0.90686				
6	0.90980	0.90718	0.90688					
7	0.90867	0.90701						
8	0.90800							
				(b)				
1	0.25	0.20744	0.19183	0.18416	0.17986	0.17726	0.17562	0.17455
2	0.20843	0.18425	0.17788	0.17513	0.17379	0.17310	0.17273	
3	0.19285	0.17794	0.17433	0.17312	0.17263	0.17244		
4	0.18506	0.17521	0.17313	0.17254	0.17238			
5	0.18061	0.17386	0.17264	0.17238				
6	0.17788	0.17315	0.17244					
7	0.17611	0.17276						
8	0.17494							

Section III B will report on a large-k resummation procedure and compare it with the Monte Carlo results of Sec. II.

B. Summation of the perturbative expansion in the large-k regime

In this section we assume that the long k-mer limit of the jamming coverage does not vanish, as shown by our simulation results.

Let us first discuss the connection between adsorption of line segments by a one-dimensional lattice and adsorption by a two-dimensional one, as already suggested in Sec. II. Line segment deposition on a square lattice contains obviously line segment deposition on each of the one-dimensional sublattices and in the correlation between these two competing (horizontal and vertical) adsorptions resides the difficulty of the study. Owing to the flux definition used in Eq. (3), the one-dimensional coverage $\Theta_1(k,t)$ appears explicitly in both lattice directions as one special configuration among all the others because one has to sum over all possible relative orientations of the segments. This is perturbatively observed on the time series of the coverage in which $2\Theta_1(k,t)$ sums up all the terms in k and k^2. Moreover we can rewrite Eq. (7) as

$$\Theta(k,t) \simeq 2kt \sum_{n\geq 0} \tilde{N}_n \quad (k^2 t)^n, \quad k \gg 1, \tag{8}$$

which then shows two kinds of "scaling" variables: kt, typical of a one-dimensional RSA of k-mers, and a second one, $k^2 t$.

Therefore we define a "correlation" function by

$$\Gamma(k,t) = \frac{\Theta(k,t)}{2\Theta_1(k,t)} \quad . \tag{9}$$

Using the results from the Monte Carlo simulation of Table I and from the series Eq. (6), inserting the exactly known one-dimensional coverage $\Theta_1(k,t)$, we can give the following properties of $\Gamma(k,t)$, which illustrate its smooth behavior: (i) $\Gamma(k,0) = 1 \ \forall \ k$; (ii) $\Gamma(k,\infty)$, which is related to the jamming coverage, varies slowly with k [e.g., $\Gamma(k,\infty) = 1/2, 0.524, 0.514, 0.504, \ldots, 0.444$ for $k = 1,2,3,4,\ldots,\infty$]; (iii) we can define a scaling variable $u = k^2 t$ in such a way that the coefficients of the power series in u of $\Gamma(k,u)$ are slowly varing polynomials in $1/k$, as it can be seen from the first terms of $\Gamma(k,u)$

$$\Gamma(k,u) = 1 - \frac{u}{2} + \left(1 + \frac{1}{k} - \frac{5}{4k^2}\right)\frac{u^2}{3} + \cdots .$$

Collecting the subseries in u of a given power of $1/k$ in $\Gamma(k,u)$ we then define

$$\Gamma(k,u) = \Gamma(\infty,u) \left(1 + \frac{G_1(u)}{k} + \frac{G_2(u)}{k^2} + \cdots\right), \tag{10}$$

which has to be understood as an asymptotic expansion of $\Gamma(k,u)$ when k goes to infinity, as long as the various series in u appearing in Eq. (10) can be resummed, and in particular

$$\Gamma(\infty,u) = 1 - \frac{1}{2}u + \frac{1}{3}u^2 - \frac{23}{108}u^3 + \frac{283}{2160}u^4 - \frac{50\,593}{648\,000}u^5 + \frac{264\,017}{5\,832\,000}u^6 + O(u^7). \tag{11}$$

In the following we shall work out a resummation procedure for $\Gamma(\infty, u)$ together with an evaluation of the subleading terms in $1/k$, and we find sensible results.

A quick glance at the perturbative expansion of $\Gamma(\infty, u)$ given by Eq. (11) reveals its striking similarity with the expansion of $\ln(1+u)/u$, starting with an identity of the first three terms. Therefore we write

$$\Gamma(\infty, u) = \frac{\ln[1+\Phi(u)]}{\Phi(u)} \tag{12}$$

in which the perturbative expansion of $\Phi(u)$ can be easily obtained from Eqs. (11) and (12).

The final task is to find the limit at $u = \infty$ of Φ. We have used a standard method for such an extrapolation, namely a mapping $v(u)$ of the u variable followed by a Padé analysis of the v series. In practice we have searched for intersections of Padé approximants by varying the parameter α entering the definition of the mapping

$$v(u) = \frac{1 - e^{-\alpha u}}{\alpha}$$

after the approximants have been calculated at the point $v = 1/\alpha$. From these intersections leading to the evaluation of $\Phi(\infty)$ we finally obtain $\theta(\infty, \infty)$.

Figure 5 shows the Padé intersections in the plane (θ, α). The multiple intersections (of the fifth and sixth order) group into four nearby classes in which we select those containing the approximants of the highest order by $\Theta = 0.658$ and $\Theta = 0.670$ and thus we deduce our result for the coverage of a square lattice by infinitely long line segments

$$\Theta(\infty, \infty) = 0.664(6) \quad ,$$

in good agreement with the Monte Carlo value, $\Theta = 0.660(2)$ obtained in Sec. II.

Let us now briefly describe the time-series computation

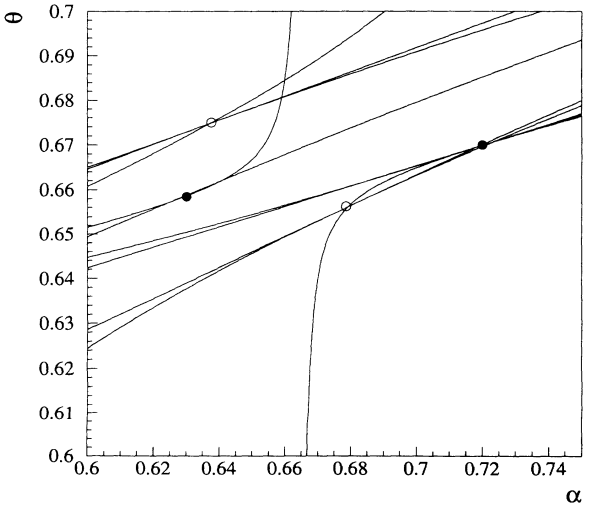

FIG. 5. Padé approximants plot of the fifth and sixth order versus the variational parameter α. Intersections of Padé approximants of the sixth order are shown by full circles, whereas open circles are located at the other intersections.

of the subleading coefficients A_1 and A_2, which appear in the asymptotic expansion of the jamming coverage

$$\Theta(k, \infty) = \Theta(\infty, \infty) + \frac{A_1}{k} + \frac{A_2}{k^2} + \cdots \quad .$$

We have applied the same mapping and Padé analysis as above on the subdominant series $G_1(u)$ and $G_2(u)$ defined by Eq. (10). Among the distinct solutions that we have obtained, namely

$$(G_1(\infty), \alpha) = \{(0.956, 0.887), (0.713, 1.165), (1.889, 0.333)\}$$

and

$$(G_2(\infty), \alpha) = \{(-1.377, 0.694), (-0.791, 1.368)\},$$

the preferred solution, which corresponds to a larger number of intersecting central approximants, has been quoted first. These values of $G_1(\infty)$ and $G_2(\infty)$ and the known asymptotic behavior of $\Theta_1(k, \infty)$ [15] allow us to finally give our preferred estimates for A_1 and A_2

$$A_1 = 0.827, \qquad A_2 = -0.699$$

together with the global range we have obtained from this method

$$0.6 \le A_1 \le 1.5, \qquad -0.8 \le A_2 \le -0.1 \quad .$$

This result compares well to the best fit of our Monte Carlo data from Eq. (1), except for A_2 , found to be too small. As a consistency check of the $1/k$ expansion we have also resummed $\Gamma(k, u)$ for finite values of k using the same method as for $\Gamma(\infty, u)$. We find essentially the same kind of results, which only differ by few percent from our asymptotic calculation, which is

$$\theta(k, \infty) = 0.664 + \frac{0.827}{k} - \frac{0.699}{k^2} \quad ,$$

and gives an unexpected precision of the coverage at all k values. Actually it deviates from the simulation data of Table I at most by 2%, reached at $k = 4$, in the whole k range.

In conclusion we have shown that the perturbative expansion summation of long k-mer coverage can be brought into full agreement with the Monte Carlo simulations.

IV. CONCLUSION

We have determined the saturation coverage of randomly adsorbed segments on a square lattice as a function of the size of the segments, by two independent methods: a numerical simulation and a time-series resummation method. Its behavior for large segments has been obtained and both methods give comparable results both for the asymptotic value itself and for the approach to this limit. Indications that the large-segment deposition process is driven by a one-dimensional mechanism have been seen in both cases, on the one hand, through linear fluctutations in the simulation and, on the other, by the particular role played by the one-dimensional cov-

erage time series that we used in the resummation of the two-dimensional one.

Actually, a simple argument may explain this fact. If one assumes that a jammed configuration is translationally invariant (in average) and invariant versus the exchange of the X and Y axes, it is sufficient to determine the coverage of *a single line* of the system to get the total coverage. On a line, the occupied sites are distributed among segments and points which result from the intersection of the line with transversely deposited segments. For instance, in the jammed configurations, a local order is clearly apparent due to the tendency of the last deposited segment to align with previously deposited ones. By measuring the distribution of cluster sizes for the points and the gaps on the line, one would guess a one-dimensional process to approximate the true bi-dimensional one. If this were indeed true, it would be possible to derive some simple approximations for the correlations functions. We plan to investigate this aspect of the model in the future.

ACKNOWLEDGMENTS

The Laboratoire de Physique Théorique is "Unité associée au Centre National de la Recherche Scientifique No. 764."

[1] J.W. Evans, Rev. Mod. Phys. (to be published).
[2] M.C. Bartelt and V. Privman, Int. J. Mod. Phys. **B5**, 2883 (1991).
[3] P.J. Flory, J. Am. Chem. Soc. **61**, 1518 (1939).
[4] A. Renyi, Publ. Math. Inst. Hung. Acad. Sci. **3**, 109 (1958).
[5] V. Privman, J.-S. Wang, and P. Nielaba, Phys. Rev. B **43**, 3366 (1991).
[6] B.J. Brosilow, R.M. Ziff, and R.D. Vigil, Phys. Rev. A **43**, 631 (1991).
[7] J.D. Sherwood, J. Phys. A **23**, 2827 (1990).
[8] R.D. Vigil and R.B. Ziff, J. Chem. Phys. **91**, 2599 (1989).
[9] J. Talbot, G. Tarjus, and P. Schaaf, Phys. Rev. A **40**, 4808 (1989).
[10] R.M. Ziff and R.D. Vigil, J. Phys. A **23**, 5103 (1990).
[11] G. Tarjus and P. Viot, Phys. Rev. Lett. **67**, 1875 (1991).
[12] P. Viot, G. Tarjus, S.M. Ricci and J. Talbot, Physica A, **191**, 248 (1992).
[13] S.S. Manna and N.M. Švrakić, J. Phys. A **24**, L671 (1991).
[14] J.P. Aimé (private communication).
[15] J.K. MacKenzie, J. Chem. Phys. **37**, 723 (1962).
[16] M.C. Bartelt, Phys. Rev. A **43**, 3149 (1991).
[17] R.S. Nord, J. Stat. Comput. Simul. **39**, 231 (1991).
[18] R.S. Nord, J. Math. Chem. (to be published). R.W. Freedman and F. Gornick (unpublished).
[19] Y. Fan and J.K. Percus, Phys. Rev. A **44**, 5099 (1991).
[20] R. Dickman, J.S. Wang, and J. Jensen, J. Chem. Phys. **94**, 8252 (1991).
[21] B. Bonnier, M. Hontebeyrie, and C. Meyers, Physica A **198**, 1 (1993).
[22] G. Tarjus, P. Schaaf, and J. Talbot, J. Stat. Phys. **63**, 167 (1991).
[23] W.G. Hoover and A.G. DeRocco, J. Chem. Phys. **36**, 3141 (1962).
[24] J.W. Evans and R.S. Nord, J. Stat. Phys. **38**, 681 (1985).